Copyright © 2009 Tech Science Press CMC, vol.9, no.2, pp.93-109, 2009

Construction of Green's function using null-field integral approach for Laplace problems with circular boundaries

Jeng-Tzong Chen[1,2], **Jia-Nan Ke**[1] **and Huan-Zhen Liao**[1]

Abstract: A null-field approach is employed to derive the Green's function for boundary value problems stated for the Laplace equation with circular boundaries. The kernel function and boundary density are expanded by using the degenerate kernel and Fourier series, respectively. Series-form Green's function for interior and exterior problems of circular boundary are derived and plotted in a good agreement with the closed-form solution. The Poisson integral formula is extended to an annular case from a circle. Not only an eccentric ring but also a half-plane problem with an aperture are demonstrated to see the validity of the present approach. Besides, a half-plane problem with a circular hole subject to Dirichlet and Robin boundary conditions and a half-plane problem with a circular hole and a semi-circular inclusion are solved. Good agreement is made after comparing with the Melnikov's results.

Keywords: degenerate kernel, Fourier series, Green's function, null-field approach and Poisson integral formula.

1 Introduction

Green's function has been studied and applied in many fields by mathematicians as well as engineers [Jaswon and Symm (1977); Melnikov (1977); Yang and Tewary (2008); Yang, Wong and Qu (2008)]. According to the superposition principle, the problems with distributed loading can be easily solved. The main difference from the fundamental solution (free-space Green's function) is that it not only satisfies the governing equation with a concentrated source but also matches the boundary condition of bounded domain. Poisson integral formula was constructed after the special Green's function is obtained. It is well known that the kernel function in the Poisson integral formula is the normal derivative of the Green's function

[1] Department of Harbor and River Engineering, National Taiwan Ocean University, Keelung, Taiwan
[2] Department of Mechanical and Mechatronic Engineering, National Taiwan Ocean University, Keelung, Taiwan. Email: jtchen@mail.ntou.edu.tw

for the Dirichlet problem of a circle. For deriving the Green's function, Thomson [Thomson (1848)] proposed the concept of reciprocal radii to find the image source to satisfy the homogeneous Dirichlet boundary condition. A Green's function for a continuously non-homogeneous saturated media has been presented [Seyrafian, Gatmiri and Noorzad (2006)]. On the other hand, Chen and Wu [Chen and Wu (2006)] proposed an alternative way to find the location of image through the degenerate kernel. For a complicated domain, the closed-form Green's function as well as series form is not easy to obtain. Analytical Green's functions have been presented for only a few configurations in two-dimensional applications and require complex variable theory. Numerical Green's function has received attention from BEM researchers by Telles et al. [Telles, Castor and Guimaraes (1995); Guimaraes and Telles (2000); Ang and Telles (2004); Melnikov (2001)]. Melnikov used the method of modified potential (MMP) to calculate the Green's function of eccentric ring and half-plane problems with a circular boundary. Boley [Boley (1956)] analytically constructed the Green's function by using the successive approximation. Adewale [Adewale (2006)] proposed an analytical solution for an annular plate subjected to a concentrated load which also belongs to the Green's function.

In this paper, we focus on the null-field approach to determine the Green's function for problems with circular boundaries. Green's functions for annular, eccentric case and half-plane problems with a circular hole or an aperture and a semi-circular inclusion are found semi-analytically. Analytical and semi-analytical solutions for the annular case are checked by each other. The results of eccentric case and half-plane problems with a circular hole or an aperture and a semi-circular inclusion are compared with those by Melnikov.

2 Derivation of the Green's function for Laplace problems with circular boundaries

2.1 Problem statement and null-field integral approach to construct the Green's function

For a two-dimensional problem with circular boundaries as shown in Fig. 1, the Green's function satifies

$$\nabla^2 G(x,\xi) = \delta(x-\xi), \quad x \in D, \tag{1}$$

where D is the domain and $\delta(x-\xi)$ denotes the Dirac-delta function of source at ξ. For simplicity, this problem is subject to the Dirichlet boundary condition

$$G(x,\xi) = 0, \quad x \in B, \tag{2}$$

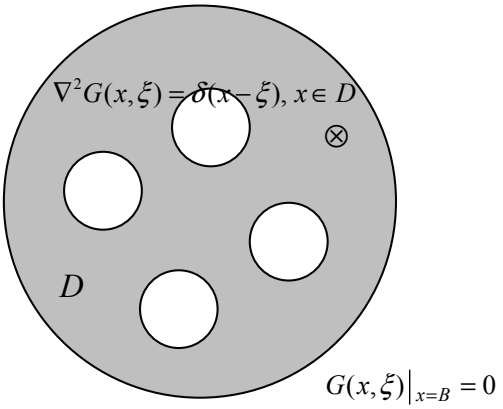

Figure 1: Green's function for a Laplace problem with circular boundaries

where B is the boundary. In order to employ the Green's third identity [Rashed (2004)] as follows

$$\iint_D [u(x)\nabla^2 v(x) - v(x)\nabla^2 u(x)]dD(x) = \int_B [(u(x)\frac{\partial v(x)}{\partial n} - v(x)\frac{\partial u(x)}{\partial n}]dB(x), \tag{3}$$

we need two systems, $u(x)$ and $v(x)$. We choose $u(x)$ as $G(x,\xi)$ and set $v(x)$ as the fundamental solution $U(x,s)$ such that

$$\nabla^2 U(x,s) = 2\pi\delta(x-s). \tag{4}$$

Then, we can obtain the fundamental solution as follows

$$U(s,x) = \ln r, \tag{5}$$

where r is the distance between s and x ($r \equiv |x-s|$).
After exchanging with the variables x and s, we have

$$2\pi G(x,\xi) = \int_B T(s,x)G(s,\xi)dB(s) - \int_B U(s,x)\frac{\partial G(s,\xi)}{\partial n_s}dB(s) + U(\xi,x), \tag{6}$$

where $T(s,x)$ is defined by

$$T(s,x) \equiv \frac{\partial U(s,x)}{\partial n_s}, \tag{7}$$

in which n_s denotes the outward normal vector at the source point s. To solve the above equation, we utilize the null-field integral equation to derive the Green's function. To solve the unknown boundary density $\partial G/\partial n_s$, the field point x is located outside the domain to yield the null-field integral equation as shown below:

$$0 = \int_B T(s,x)G(s,\xi)dB(s) - \int_B U(s,x)\frac{\partial G(s,\xi)}{\partial n_s}dB(s) + U(\xi,x), \quad x \in D^c \tag{8}$$

where D^c is the complementary domain. By using the degenerate kernels, the BIE for the "boundary point" can be easily derived through the null-field integral equation by exactly collocating x on B in Eq. (8) [Chen, Shen and Chen (2006)].

2.2 Expansion of kernel function and boundary density

Based on the separable property, the kernel function $U(s,x)$ can be expanded into series form by separating the field point $x(\rho,\phi)$ and source point $s(R,\theta)$ in the polar coordinates:

$$U(s,x) = \begin{cases} U^i(R,\theta;\rho,\phi) = \ln R - \sum\limits_{m=1}^{\infty} \frac{1}{m}\left(\frac{\rho}{R}\right)^m \cos m(\theta-\phi), & R \geq \rho \\ U^e(R,\theta;\rho,\phi) = \ln \rho - \sum\limits_{m=1}^{\infty} \frac{1}{m}\left(\frac{R}{\rho}\right)^m \cos m(\theta-\phi), & \rho > R \end{cases} \tag{9}$$

It is noted that the leading term and the denominator in the above expansion involve the larger argument to ensure the log singularity and the series convergence, respectively. According to the definition of $T(s,x)$in Eq. (7), we have

$$T(s,x) = \begin{cases} T^i(R,\theta;\rho,\phi) = \frac{1}{R} + \sum\limits_{m=1}^{\infty} (\frac{\rho^m}{R^{m+1}}) \cos m(\theta-\phi), & R > \rho \\ T^e(R,\theta;\rho,\phi) = -\sum\limits_{m=1}^{\infty} (\frac{R^{m-1}}{\rho^m}) \cos m(\theta-\phi), & \rho > R \end{cases} \tag{10}$$

The unknown boundary densities can be represented by using the Fouries series as shown below:

$$G(s_k,\xi) = a_0^k + \sum_{n=1}^{\infty} (a_n^k \cos n\theta_k + b_n^k \sin n\theta_k), \quad s_k \in B_k,\ k = 1,2,\cdots,N, \tag{11}$$

$$\frac{\partial G(s_k,\xi)}{\partial n_s} = p_0^k + \sum_{n=1}^{\infty} (p_n^k \cos n\theta_k + q_n^k \sin n\theta_k),, \quad s_k \in B_k,\ k = 1,2,\cdots,N, \tag{12}$$

where N is the number of circular boundaries. In real computation, the finite number of M terms for expansion of kernel and boundary density are adopted.

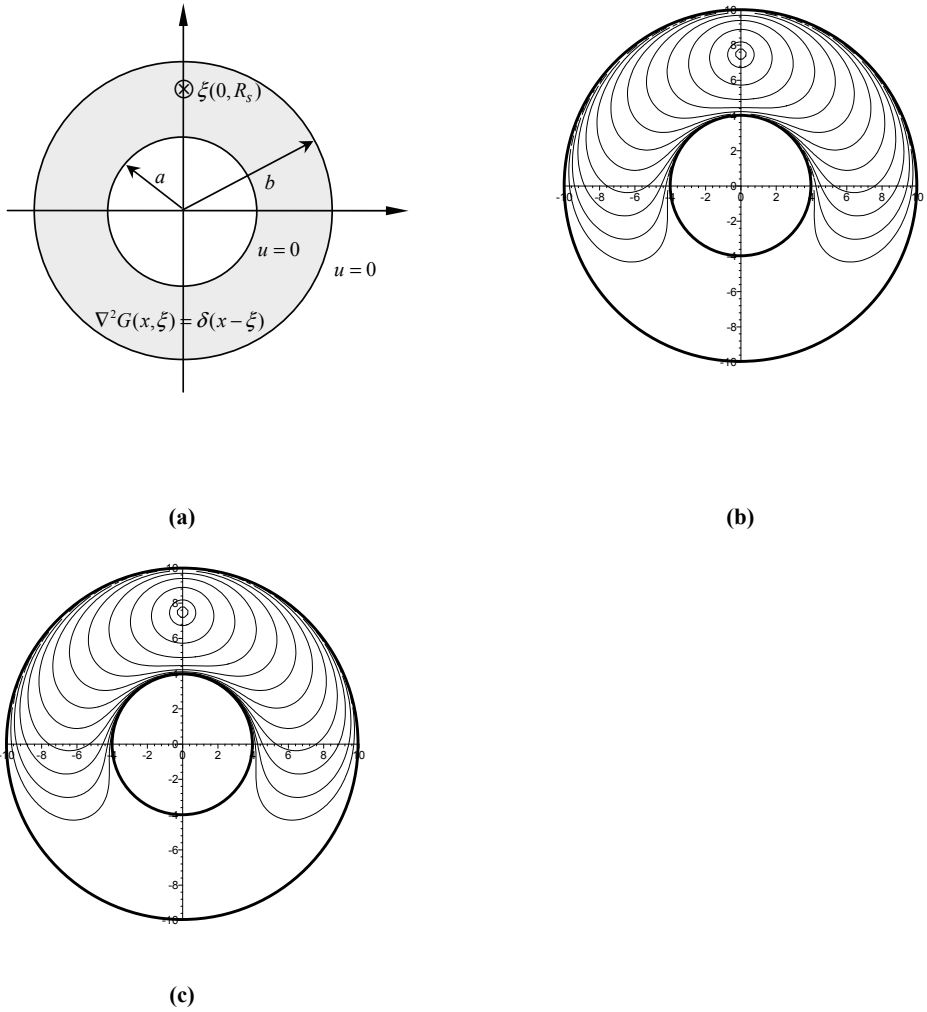

Figure 2: (a): Problem statement of Green's function for annular case; (b): Green's function for the annular case (analytical solution, M=50); (c): Green's function for the annular case (semi-analytical solution, M=50)

3 Series representation for the Green's function of annular case

For the annular case as shown in Fig. 2(a) subject to the Dirichlet boundary condition, the unknown Fourier series can be analytically derived. By collocating x on

(b^+,ϕ) and (a^-,ϕ), the null-field equations yield

$$0=(1-2\pi bp_0-2\pi a\bar{p}_0)\ln b$$
$$-\sum_{m=1}^{\infty}\frac{1}{m}\{[b\pi p_m+a\pi(\frac{a}{b})^m\bar{p}_m+(\frac{R_s}{b})^m\cos m\theta_s]\cos m\phi$$
$$+[b\pi q_m+a\pi(\frac{a}{b})^m\bar{q}_m+(\frac{R_s}{b})^m\sin m\theta_s]\sin m\phi\},x\to(b^+,\phi) \quad (13)$$

$$0=(\ln R_s-2\pi b\ln bp_0-2\pi a\ln a\ \bar{p}_0)$$
$$-\sum_{m=1}^{\infty}\frac{1}{m}\{[b\pi(\frac{a}{b})^m p_m+a\pi\bar{p}_m+(\frac{a}{R_s})^m\cos m\theta_s]\cos m\phi$$
$$+[b\pi(\frac{a}{b})^m q_m+a\pi\bar{q}_m+(\frac{a}{R_s})^m\sin m\theta_s]\sin m\phi\},x\to(a^-,\phi) \quad (14)$$

where a and b are the inner and outer radii, respectively. For the Dirichlet case, the explicit form for the unkown Fourier series can be obtained as

$$\begin{Bmatrix}p_0\\ \bar{p}_0\end{Bmatrix}=\begin{Bmatrix}\frac{\ln a-\ln R_s}{2\pi b(\ln a-\ln b)}\\ \frac{\ln b-\ln R_s}{2\pi a(\ln b-\ln a)}\end{Bmatrix} \quad (15)$$

$$\begin{Bmatrix}p_m\\ \bar{p}_m\end{Bmatrix}=\begin{Bmatrix}\frac{b^{m-1}\cos m\theta_s[b^m(\frac{R_s}{b})^m-a^m(\frac{a}{R_s})^m]}{(b^{2m}-a^{2m})\pi}\\ \frac{b^m\cos m\theta_s[b^m(\frac{a}{R_s})^m-a^m(\frac{R_s}{b})^m]}{a(b^{2m}-a^{2m})\pi}\end{Bmatrix} \quad (16)$$

$$\begin{Bmatrix}q_m\\ \bar{q}_m\end{Bmatrix}=\begin{Bmatrix}\frac{b^{m-1}\sin m\theta_s[b^m(\frac{R_s}{b})^m-a^m(\frac{a}{R_s})^m]}{(b^{2m}-a^{2m})\pi}\\ \frac{b^m\sin m\theta_s[b^m(\frac{a}{R_s})^m-a^m(\frac{R_s}{b})^m]}{a(b^{2m}-a^{2m})\pi}\end{Bmatrix} \quad (17)$$

where p_m, q_m, $\bar{p}_m$ and $\bar{q}_m$ are the Fourier coefficients of boundary densities for normal flux as shown below:

$$t(s)=\sum_{m=0}^{\infty}(\bar{p}_m\cos m\theta+\bar{q}_m\sin m\theta),\ s\in\text{inner boundary} \quad (18)$$

$$t(s)=\sum_{m=0}^{\infty}(p_m\cos m\theta+q_m\sin m\theta),\ s\in\text{outer boundary} \quad (19)$$

By substituting all the boundary densities into the integral representation for the domain point, we have the series-form Green's function as shown below:

$$G(x,\xi) = -(b\ln b\ p_0 + a\ln\rho\ \bar{p}_0) + \sum_{m=1}^{\infty}\frac{1}{2m}\{[b(\frac{\rho}{b})^m p_m + a(\frac{a}{\rho})^m \bar{p}_m]\cos m\phi + [b(\frac{\rho}{b})^m q_m + a(\frac{a}{\rho})^m \bar{q}_m]\sin m\phi\} + \frac{\ln|x-\xi|}{2\pi}, \quad a \le \rho \le b \tag{20}$$

If we expand the $\ln|x-\xi|$ function, we have

$$G(x,\xi) = -(b\ln b p_0 + a\ln\rho\,\bar{p}_0 - \frac{\ln\rho}{2\pi}) + \sum_{m=1}^{\infty}\frac{1}{2m}\{[b(\frac{\rho}{b})^m p_m + a(\frac{a}{\rho})^m \bar{p}_m - (\frac{R_s}{\rho})^m\frac{\cos m\theta_s}{\pi}]\cos m\phi + [b(\frac{\rho}{b})^m q_m + a(\frac{a}{\rho})^m \bar{q}_m - (\frac{R_s}{\rho})^m\frac{\sin m\theta_\xi}{\pi}]\sin m\phi\}, \quad R_s \le \rho \le b \tag{21}$$

$$G(x,\xi) = -(b\ln b\ p_0 + a\ln\rho\ \bar{p}_0 - \frac{\ln R_s}{2\pi}) + \sum_{m=1}^{\infty}\frac{1}{2m}\{[b(\frac{\rho}{b})^m p_m + a(\frac{a}{\rho})^m \bar{p}_m - (\frac{\rho}{R_s})^m\frac{\cos m\theta_s}{\pi}]\cos m\phi + [b(\frac{\rho}{b})^m q_m + a(\frac{a}{\rho})^m \bar{q}_m - (\frac{\rho}{R_s})^m\frac{\sin m\theta_\xi}{\pi}]\sin m\phi\}, \quad a \le \rho \le R_s \tag{22}$$

Also, two limiting cases are our concern. One is the interior case of a to zero and the other is the exterior case of b to infinity. Now we move to solve the solution $w(x)$ for the following partial differential equation

$$\nabla^2 w(x) = 0, \quad x \in D, \tag{23}$$

subject to the following Dirichlet boundary condition

$$w(x) = f(x), \quad x \in \text{ inner boundary } B_1 \tag{24}$$

$$w(x) = g(x), \quad x \in \text{ outer boundary } B_2 \tag{25}$$

To extend the Poisson integral formula to an annular case for Eq. (20) subject to BCs of Eqs. (24) and (25), we have

$$2\pi w(x) = \int_{B_1+B_2} \frac{\partial G(s,x)}{\partial n_s} w(s)\,dB(s) \tag{26}$$

where $G(s,x)$ is the derived Green's function of Eq. (20). Equation (26) indicates the representation for the solution in terms of general Poisson integral formula.

Although the series-form Green's function for an annular case is derived analytically in the section, general Green's functions can be solved semi-analytically as shown in the following section.

4 Linear algebraic equation

By moving the null-field point x_j to the jth circular boundary in the limiting sense for Eq. (8), we have the linear algebraic equation

$$[\mathbf{U}]\{\mathbf{t}\} = [\mathbf{T}]\{\mathbf{u}\} + \{\mathbf{b}\}, \tag{27}$$

where $\{\mathbf{b}\}$ is the vector due to the source of Green's function, $[\mathbf{U}]$ and $[\mathbf{T}]$ are the influence matrices with a dimension of $(N+1)(2M+1)$ by $(N+1)(2M+1)$, $\{\mathbf{u}\}$ and $\{\mathbf{t}\}$ denote the column vectors of Fourier coefficients with a dimension of $(N+1)(2M+1)$ by 1 in which $[\mathbf{U}]$, $[\mathbf{T}]$, $\{\mathbf{u}\}$, $\{\mathbf{t}\}$ and $\{\mathbf{b}\}$ can be defined as follows:

$$[\mathbf{U}] = \begin{bmatrix} \mathbf{U}_{00} & \mathbf{U}_{01} & \cdots & \mathbf{U}_{0N} \\ \mathbf{U}_{10} & \mathbf{U}_{11} & \cdots & \mathbf{U}_{1N} \\ \vdots & \vdots & \ddots & \vdots \\ \mathbf{U}_{N0} & \mathbf{U}_{N1} & \cdots & \mathbf{U}_{NN} \end{bmatrix}, \quad [\mathbf{T}] = \begin{bmatrix} \mathbf{T}_{00} & \mathbf{T}_{01} & \cdots & \mathbf{T}_{0N} \\ \mathbf{T}_{10} & \mathbf{T}_{11} & \cdots & \mathbf{T}_{1N} \\ \vdots & \vdots & \ddots & \vdots \\ \mathbf{T}_{N0} & \mathbf{T}_{N1} & \cdots & \mathbf{T}_{NN} \end{bmatrix}, \tag{28}$$

$$\{\mathbf{u}\} = \begin{Bmatrix} \mathbf{u}_0 \\ \mathbf{u}_1 \\ \mathbf{u}_2 \\ \vdots \\ \mathbf{u}_N \end{Bmatrix}, \quad \{\mathbf{t}\} = \begin{Bmatrix} \mathbf{t}_0 \\ \mathbf{t}_1 \\ \mathbf{t}_2 \\ \vdots \\ \mathbf{t}_N \end{Bmatrix}, \quad \{\mathbf{b}\} = \begin{Bmatrix} \mathbf{b}_0 \\ \mathbf{b}_1 \\ \mathbf{b}_2 \\ \vdots \\ \mathbf{b}_N \end{Bmatrix} \tag{29}$$

where the vectors $\{\mathbf{u}_k\}$ and $\{\mathbf{t}_k\}$ are in the form of $\left\{a_0^k \quad a_1^k \quad b_1^k \quad \cdots \quad a_M^k \quad b_M^k\right\}^T$ and $\left\{p_0^k \quad p_1^k \quad q_1^k \quad \cdots \quad p_M^k \quad q_M^k\right\}^T$ respectively; the first subscript "j" (j = 0, 1, 2, ..., N) in $\left[\mathbf{U}_{jk}\right]$ and $\left[\mathbf{T}_{jk}\right]$ denotes the index of the jth circle where the collocation point is located and the second subscript "k" ($k = 0, 1, 2, \cdots, N$) denotes the index of the kth circle where boundary data $\{\mathbf{u}_k\}$ or $\{\mathbf{t}_k\}$ are specified, N is the number of circular holes in the domain and M indicates the truncated terms of Fourier series. The coefficient matrix of the linear algebraic system is partitioned into blocks, and each off-diagonal block corresponds to the influence matrices between two different circular cavities. The diagonal blocks are the influence matrices due to itself in each individual hole. After uniformly collocating the point along the kth circular

boundary, the submatrix can be written as

$$\left[\mathbf{U}_{jk}\right] = \begin{bmatrix} U_{jk}^{0c}(\phi_1) & U_{jk}^{1c}(\phi_1) & U_{jk}^{1s}(\phi_1) \\ U_{jk}^{0c}(\phi_2) & U_{jk}^{1c}(\phi_2) & U_{jk}^{1s}(\phi_2) \\ U_{jk}^{0c}(\phi_3) & U_{jk}^{1c}(\phi_3) & U_{jk}^{1s}(\phi_3) \\ \vdots & \vdots & \vdots \\ U_{jk}^{0c}(\phi_{2M}) & U_{jk}^{1c}(\phi_{2M}) & U_{jk}^{1s}(\phi_{2M}) \\ U_{jk}^{0c}(\phi_{2M+1}) & U_{jk}^{1c}(\phi_{2M+1}) & U_{jk}^{1s}(\phi_{2M+1}) \end{bmatrix} \begin{bmatrix} \cdots & U_{jk}^{Mc}(\phi_1) & U_{jk}^{Ms}(\phi_1) \\ \cdots & U_{jk}^{Mc}(\phi_2) & U_{jk}^{Ms}(\phi_2) \\ \cdots & U_{jk}^{Mc}(\phi_3) & U_{jk}^{Ms}(\phi_3) \\ \ddots & \vdots & \vdots \\ \cdots & U_{jk}^{Mc}(\phi_{2M}) & U_{jk}^{Ms}(\phi_{2M}) \\ \cdots & U_{jk}^{Mc}(\phi_{2M+1}) & U_{jk}^{Ms}(\phi_{2M+1}) \end{bmatrix} \tag{30}$$

$$\left[\mathbf{T}_{jk}\right] = \begin{bmatrix} T_{jk}^{0c}(\phi_1) & T_{jk}^{1c}(\phi_1) & T_{jk}^{1s}(\phi_1) \\ T_{jk}^{0c}(\phi_2) & T_{jk}^{1c}(\phi_2) & T_{jk}^{1s}(\phi_2) \\ T_{jk}^{0c}(\phi_3) & T_{jk}^{1c}(\phi_3) & T_{jk}^{1s}(\phi_3) \\ \vdots & \vdots & \vdots \\ T_{jk}^{0c}(\phi_{2M}) & T_{jk}^{1c}(\phi_{2M}) & T_{jk}^{1s}(\phi_{2M}) \\ T_{jk}^{0c}(\phi_{2M+1}) & T_{jk}^{1c}(\phi_{2M+1}) & T_{jk}^{1s}(\phi_{2M+1}) \end{bmatrix} \begin{bmatrix} \cdots & T_{jk}^{Mc}(\phi_1) & T_{jk}^{Ms}(\phi_1) \\ \cdots & T_{jk}^{Mc}(\phi_2) & T_{jk}^{Ms}(\phi_2) \\ \cdots & T_{jk}^{Mc}(\phi_3) & T_{jk}^{Ms}(\phi_3) \\ \ddots & \vdots & \vdots \\ \cdots & T_{jk}^{Mc}(\phi_{2M}) & T_{jk}^{Ms}(\phi_{2M}) \\ \cdots & T_{jk}^{Mc}(\phi_{2M+1}) & T_{jk}^{Ms}(\phi_{2M+1}) \end{bmatrix} \tag{31}$$

$$\left\{\mathbf{b}_j\right\} = \begin{Bmatrix} \ln\left|\mathbf{x}(\rho_j,\phi_1) - \xi\right| \\ \ln\left|\mathbf{x}(\rho_j,\phi_2) - \xi\right| \\ \ln\left|\mathbf{x}(\rho_j,\phi_3) - \xi\right| \\ \vdots \\ \ln\left|\mathbf{x}(\rho_j,\phi_{2M+1}) - \xi\right| \end{Bmatrix} \tag{32}$$

where the influence coefficients are explicitly expressed as

$$U_{jk}^{nc}(\phi_m) = \int_{B_k} U(s_k, x_m)\, \cos(n\theta_k)\, R_k d\theta_k, \tag{33}$$

$$U_{jk}^{ns}(\phi_m) = \int_{B_k} U(s_k, x_m)\, \sin(n\theta_k)\, R_k d\theta_k, \tag{34}$$

$$T_{jk}^{nc}(\phi_m) = \int_{B_k} T(s_k, x_m)\, \cos(n\theta_k)\, R_k d\theta_k, \tag{35}$$

$$T_{jk}^{ns}(\phi_m) = \int_{B_k} T(s_k, x_m)\, \sin(n\theta_k)\, R_k d\theta_k, \tag{36}$$

where $n = 0,\ 1,\ 2,\ \cdots,\ M$, $m = 1,\ 2,\ \cdots,\ 2M+1$, and ϕ_m is the polar angle of the collocating point x_m along the boundary. By rearranging the known and unknown sets, the unknown Fourier coefficients are determined. Equation (8) can be calculated by employing the relations of trigonometric function and the orthogonal property in the real computation. Only the finite number of M terms are used in the Fourier expansion of boundary densities and kernels. After obtaining the unknown Fourier coefficients, we can obtain the interior potential by employing Eq. (6).

5 Derivation of the Green's function with several circular holes and inclusions

For the problems with inclusions, we can decompose into subsystems of matrix and inclusion after taking free body on the interface. The two systems of matrix and inclusion yield

$$\left[U^M\right]\left\{t^M\right\} = \left[T^M\right]\left\{u^M\right\} \tag{37}$$

$$\left[U^I\right]\left\{t^I\right\} = \left[T^I\right]\left\{u^I\right\} + \{b\} \tag{38}$$

where the superscripts "M" and "I" denote the systems of matrix and inclusion, respectively. Two constrains of continuity for the displacement and equilibrium of force are shown below:

$$\left\{u^M\right\} = \left\{u^I\right\} \quad \text{on } B_k, \tag{39}$$

$$[-\lambda_2]\left\{t^M\right\} = [\lambda_1]\left\{t^I\right\} \quad \text{on } B_k, \tag{40}$$

where λ_1 and λ_2 represent the material conductivity of inclusion and matrix, respectively.

By assembling the matrices in Eqs. (37), (38), (39) and (40), we have

$$\begin{bmatrix} T^M & -U^M & 0 & 0 \\ 0 & 0 & T^I & -U^I \\ I & 0 & -I & 0 \\ 0 & -\lambda_2 & 0 & -\lambda_1 \end{bmatrix} \begin{bmatrix} u^M \\ t^M \\ u^I \\ t^I \end{bmatrix} = \begin{bmatrix} 0 \\ U(\xi, x) - U(\xi', x) \\ 0 \\ 0 \end{bmatrix} \tag{41}$$

The unknown coefficients in the algebraic system can be determined. Then, we can solve the potential by Eq. (6). The half-plane problem is imbedded to a full-plane problem through the image method. By employing the anti-symmetric property, the boundary condition of half-plane can be satisfied through the image approach. In the real implementation, the full-plane problem is solved, first.

6 Illustrative examples and discussions

Case 1: annular case (analytical and semi-analytical solutions).

The influence matrix is singular for the Dirichlet problem as the radius b is one. No matter what the null-field point collocated (a^- and b^+) due to the property of degenerate kernel in Eq. (9), one column of the influence matrix $[U]$ is a zero vector. For more detail, please find our recent work [Chen and Shen (2007)] for eccentric Laplace problems. Another one by Liu and Lean can be consulted [Liu and Lean (1990)]. To avoid the degenerate scale, we design the radii of inner and outer boundaries are 4 and 10. The source of the Green's function is located on $\xi = (0, 7.5)$. For the annular Green's function, both the analytical solution and the semi-analytical results are shown in Figs. 2(b) and 2(c). The analytical solution is obtained by truncating Fourier series of fifty terms in real implementation. One hundred and one collocation points along the inner and outer boundaries are used in the semi-analytical approach. Good agreement is made to verify the validity of the program using the semi-analytical procedure.

Case 2: eccentric ring (a semi-analytical solution).

Figure 3(a) depicts the Green's function of the eccentric ring. The source point is located at $\xi = (0, 0.75)$. Figures 3(b) and 3(c) show the potential distribution by using the present method and Melnikov's approach, respectively. The two radii of inner and outer circles are a=0.4 and b=1.0. The two centers of the inner and outer circles are (-0.4, 0) and (0,0), respectively. It is noted that outer radius of one is a degenerate scale and needs special treatment as described in detail by Chen and Shen. Comparison of the present results with those MCP and MMP methods is shown in Table 1. Good agreement is made.

Case 3: a half plane with an aperture (a semi-analytical solution).

Figure 4(a) depicts the Green's function for the half plane with a hole. The source point is located at $\xi = (2, 1)$. The center and radius of the aperture are $(0, 3)$ and a=1.0. Figures 4(b) and 4(c) show the potential distribution by using the present method and Melnikov's approach, respectively. Good agreement is made.

Case 4: a half-plane problem with a circular boundary subject to the Robin boundary condition.

Table 1: Comparison of the numerical results

Field point, y	MCP		MMP		Present Method		
	Partitioning number, k [Melnikov and Melnikov (2001)]				Fourier term, M		
	10	20	50	10	20	50	10	20	50
0	0.000280	0.000128	0.000067	0.000107	0.000049	0.000032	0.000000	0.000000	0.000000
0.2	0.010667	0.010712	0.010781	0.010700	0.010779	0.010798	0.010832	0.010832	0.010832
0.4	0.062359	0.062411	0.062443	0.062407	0.062435	0.062448	0.062458	0.062462	0.062462
0.6	0.177534	0.177574	0.177585	0.177583	0.177590	0.177593	0.177597	0.177596	0.177596
0.8	0.317893	0.317902	0.317911	0.317907	0.317913	0.317914	0.318032	0.317915	0.317915
1.0	0.000014	0.000006	0.000002	0.000000	0.000000	0.000000	0.002014	0.000064	0.000000

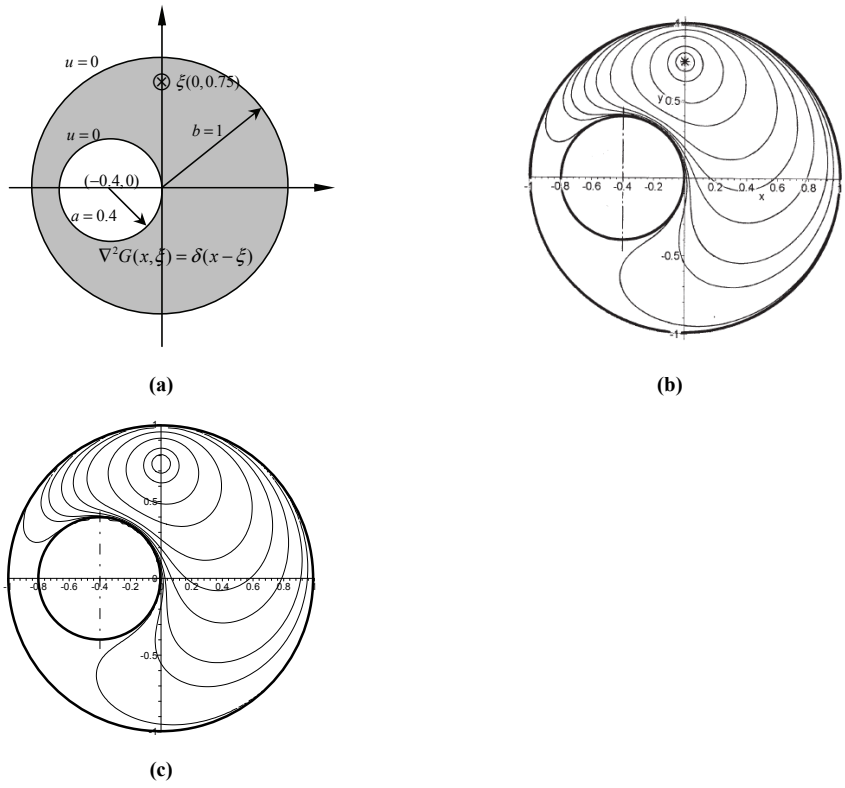

Figure 3: (a): Problem statement of Green's function for the eccentric ring; (b): Melnikov's method [Melnikov and Melnikov (2001)]; (c): Present method (M=50)

A half-plane problem with an aperture is considered. The governing equation and boundary condition are shown in Fig. 5(a). The center and radius of the aperture are $(2,2)$ and a=1.0, respectively. The Robin condition is $t = -2u$ imposed on the aperture. The concentrated source is located at $(0,3.5)$. Figures 5(b) and 5(c) show the potential distribution by using the present method and Melnikov's approach, respectively. Good agreement is obtained.

Case 5: a half plane problem with a hole and an inclusion.

A half-plane problem with a circular hole and a half-circular inclusion are considered as composed of two regions $D_1 = \{0 < r < 1,\ 0 < \varphi < \pi\}$ and $D_2 = \{1 < r < \infty,\ 0 < \varphi < \pi\}$ filled in with different materials $(\lambda = \lambda_2/\lambda_1 = 0.1)$. The governing equation and boundary condition are shown in Fig. 6(a). The center and radius of the aperture are $(r, \varphi; 1.4, \pi/3)$ and $a_2 = 0.4$, respectively. The concentrated source

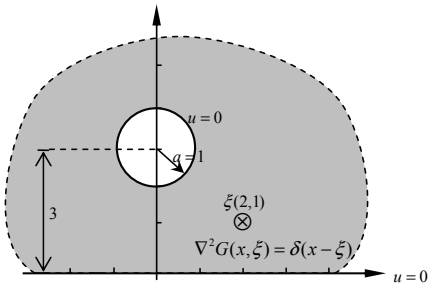

(a)

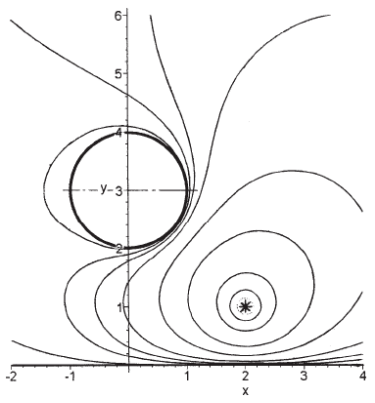

(b)

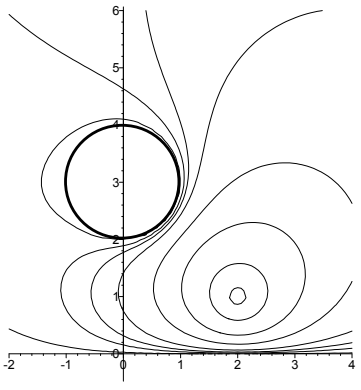

(c)

Figure 4: (a): Problem statement of Green's function for the half-plane with an aperture; (b): Melnikov's method [Melnikov and Melnikov (2001)]; (c): Present method (M=50)

is located at $(r, \varphi; 0.5, \pi/3)$. Figures 6(b) and 6(c) show the potential distribution by using the present method and Melnikov's approach, respectively. Good agreement is also made.

7 Concluding remarks

For the Green's function with circular boundaries, we have proposed a semi-analytical approach to construct the Green's function by using degenerate kernels and Fourier series. The series-form Green's function for annular Dirichlet problem is derived which can extend the Poisson integral formula from a circle to an annular case. Several examples, including the annular, eccentric cases and half plane problems with circular holes and inclusions, were demonstrated to check the validity of the

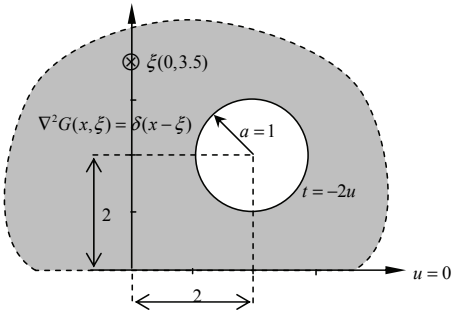

(a)

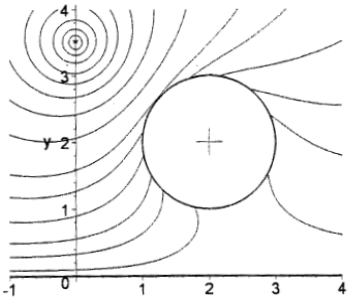

(b)

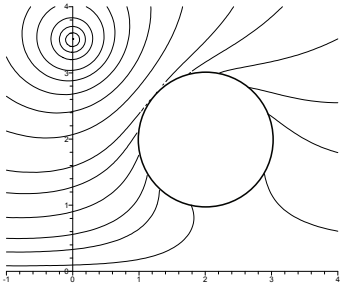

(c)

Figure 5: (a): Problem statement of Green's function for the half-plane problem with the Robin boundary condition; (b): Contour plot by using the Melnikov's approach [Melnikov and Melnikov (2006)]; (c): Contour plot by using the null-field integral equation approach (M=50)

present formulation. Our advantages are five folds: (1) mesh-free generation (2) well-posed model (3) principal value free (4) elimination of boundary-layer effect (5) exponential convergence. A general-purpose program to construct the Greem's fuction for Laplace problems with circular boundaries of arbitrary number, radius and location was implemented. Extension to construct the Green's functions for Laplace problems with circular boundaries is straightforward without any difficulty.

References

Adewale, A. O. (2006): Isotropic clamped-free thin annular plate subjected to a concentrated load. *ASME, J. Appl. Mech.*, vol.73, no.4, pp. 658-663.

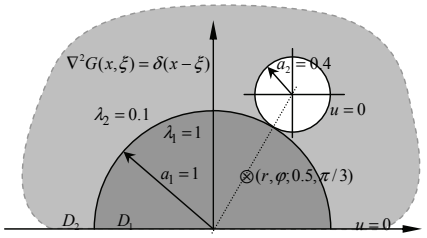

(a)

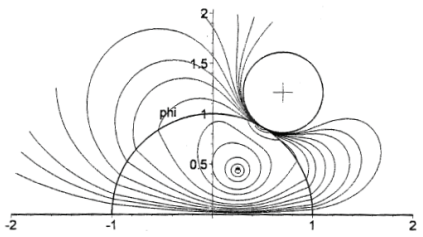

(b)

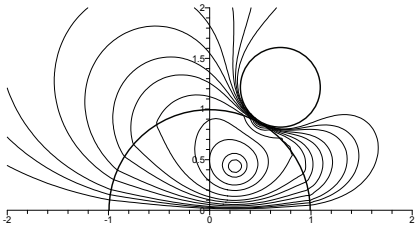

(c)

Figure 6: (a): Problem sketch of half-plane problem with a circular hole and a semi-circular inclusion; (b): Contour plot by using Melnikov's method approach [Melnikov and Melnikov (2006)]; (c): Contour plot by using the null-field integral equation approach (M=50)

Ang, W. T.; Telles, J. C. F. (2004): A numerical Green's function for multiple cracks in anisotropic bodies. *Journal of Engineering Mathematics*, vol. 49, pp. 197-207.

Boley, B. A. (1956): A method for the construction of Green's functions. *Quarterly of Applied Mathematics*, vol. 14, pp. 249-257.

Chen, J. T.; **Shen, W. C.; Chen, P. Y.** (2006): Analysis of circular torsion bar with circular holes using null-field approach. *CMES: Computer Modeling in Engineering Science*, vol. 12 (2), pp. 109-119.

Chen, J. T.; Shen, W. C. (2007): Degenerate scale for multiply connected Laplace problems. *Mechanics Research Communications,* vol. 34, pp. 69-77.

Chen, J. T.; Wu, C. S. (2006): Alternative derivations for the Poisson integral formula. *International Journal of Mathematical Education in Science and Technology*, vol. 37, pp. 165-185.

Guimaraes, S.; Telles, J. C. F. (2000): General application of numerical Green's functions for SIF computations with boundary elements. *CMES: Computer Modeling in Engineering & Sciences*, vol. 1, no. 3, pp. 131-139.

Jaswon, M. A.; Symm, G. T. (1977): Integral equation methods in potential theory and electrostatics. Academic Press, New York.

Liu, P.-L. F.; Lean, M. H. (1990): A note on Γ-contours in the integral equation formulation for a multi-connected region. In: Grilli, S., Brebbia, C. A., Cheng, A. H. D. (Eds.), *Computational Engineering with Boundary Elements*, vol. 1, pp. 295-302.

Melnikov, Y. A. (1977): Some application of the Greens' function method in mechanics. *Int. J. Solids Structures*, vol. 13, pp. 1045-1058.

Melnikov, Y. A.; Melnikov, M. Y. (2001): Modified potential as a tool for computing Green's functions in continuum mechanics. *CMES: Computer Modeling in Engineering & Sciences*, vol. 2, pp. 291-305.

Melnikov, Y. A.; Melnikov, M. Y. (2006): Green's functions for mixed boundary value problems in regions of irregular shape. *Electronic Journal of Boundary Elements*, vol. 4, pp. 82-104.

Rashed, Y. F. (2004): Green's first identity method for boundary-only solution of self-weight in BEM formulation for thick slabs. *CMC: Computers, Materials & Continua*, vol. 1, no. 4, pp. 319-326.

Seyrafian, S.; Gatmiri, B.; Noorzad, A. (2006): Green functions for a continuously non-homogeneous saturated media. *CMES: Computer Modeling in Engineering & Sciences*, vol. 15, no. 2, pp. 115-126.

Telles, J. C. F.; Castor, G. S.; Guimaraes, S. (1995): Numerical Green's function approach for boundary elements applied to fracture mechanics. *International Journal for Numerical Methods in Engineering*, vol. 38, no. 19, pp. 3259-3274.

Thomson, W. (1848): Maxwell in his treatise, vol. I., Chap. XI, quotes a paper in the Cambridge and Dublin Math. Journ. of 1848.

Yang, B.; Tewary, V. K. (2008): Green's function for multilayers with interfacial membrane and flexural rigidities. *CMC: Computers, Materials & Continua*, vol. 8, no. 1, pp. 23-31.

Yang, B.; Wong, S. C.; Qu, S.; (2008): A micromechanics analysis of nanoscale graphite platelet-reinforced epoxy using defect Green's function. *CMES: Computer Modeling in Engineering & Sciences*, vol. 24, no. 2-3, pp. 81-93.